Root morphology and biomechanical characteristics of high altitude alpine plant species and their potential application in soil stabilization

Root morphology and biomechanical characteristics of high altitude alpine plant species and their potential application in soil stabilization

C. Hudek[1,2*], C. J. Sturrock[3], B. S. Atkinson[3], S. Stanchi[1], M. Freppaz[1]

[1]University of Torino, DISAFA, Largo Paolo Braccini, 2, 10095 Grugliasco (TO), Italy

[2]T2M, Marie Curie Cofund Fellow

[3]Hounsfield Facility, School of Biosciences, The University of Nottingham, Sutton Bonington Campus, Nr Loughborough, LE12 5RD, UK

*chudek@unito.it

Abstract

Glacial forefields are young, poorly developed soils with highly unstable soil conditions. Root system contribution to soil stabilization is a well-known phenomenon. Identifying the functional traits and root morphology of pioneer vegetation that establish on forefields can lead us to useful information regarding the practical application of plants in land restoration of high altitude mountain sites.

This study aims to gather information on the root morphology and biomechanical characteristics of the 10 most dominant pioneer plant species of the forefield of Lys Glacier (NW Italian Alps).

X-ray Computed Tomography (X-ray CT) was used to visualize and quantify non-destructively the root architecture of the studied species. Samples were then cored directly from the forefield. Data on root traits such as total root length, rooting depth, root diameter, root length density and number of roots in relation to diameter classes

as well as plant height were determined and compared between species. Roots were also tested for their tensile strength resistance.

X-ray CT technology allowed us to visualize the 3D root architecture of species intact in their natural soil system. X-ray CT technology provided a visual representation of root–soil contact and information on the exact position, orientation and elongation of the root system in the soil core. Root architecture showed high variability among the studied species. For all species the majority of roots consisted of roots smaller than 0.5 mm in diameter. There were also considerable differences found in root diameter and total root length although these were not statistically significant. However, significant differences were found in rooting depth, root length density, plant height and root tensile strength between species and life forms. In all cases root tensile strength decreased with increasing root diameter. The highest tensile strength was recorded for graminoids such as *Luzula spicata* (L.) DC. and *Poa laxa* Haenke and the lowest for *Epilobium fleischeri* Hochst.

The differences in root properties among the studied species highlight the diverse adaptive and survival strategies plants employ to establish on and thrive in the harsh and unstable soil conditions of a glacier forefield. The data determined and discovered in this study could provide a significant contribution to a database that allow those who are working in land restoration and preservation of high altitude mountain sites to employ native species in a more efficient, effective and informed manner.

Keywords: alpine species; glacier forefield; root phenotyping; soil stabilization; X-ray CT

1. Introduction

Glaciers in alpine regions are affected by climate change twice as much as the global average with respect to other ecosystems (Bradley et al., 2014) which results in accelerated glacial retreat. Retreating glaciers expose young soils that are low in nutrients (carbon and nitrogen) (Bradley et al., 2014; Lazzaro et al., 2010) and highly unstable (Matthews, 1999). Mass wasting and erosion processes are common in these forefields creating an inhospitable environment for plant colonization. Vegetation establishment on glacier forefields requires species with strong adaptive strategies and with high stress and disturbance tolerances (Robbins and Matthews, 2009). In spite of the harsh environment, vegetation cover increases quickly (Matthews, 1999) due to the rapid colonization of pioneer species. Pioneer species can grow quickly on nitrogen poor soils due to their high reproduction capacity and photosynthetic activity, (Stöcklin and Bäumler, 1996) and tolerance against abiotic stresses e.g., extreme temperatures, ultraviolet radiation, atmospheric pressure, shortage of mineral nutrients (Jones and Henry, 2003 Körner, 2003; Stöcklin et al., 2009).

Successful colonization and establishment of alpine species on glacial forefields may provide important information on the practical aspects of land reclamation and habitat restoration (Robbins and Matthews, 2009). Root traits (architectural, morphological, physiological and biotic) play an important role in the physical and even though the present study will not discuss further, the chemical development of young soils (Bardgett et al., 2014; Massaccesi et al., 2015) bringing about increased structural stability in the forefield (Bardgett et al.,2014) and decreasing the frequency

and severity of any mass wasting and erosion processes. The biomechanical characteristics of roots such as tensile strength is a useful parameter for the quantification of the reinforcement potential; in particular for quantifying the added soil cohesion provided by plant roots. Determining the tensile strength of roots and their distribution in the soil profile can provide information on the increased shear strength of the soil provided by root reinforcement which can also determine plants' resilience to solifluction, frequently occurring in a periglacial environment (Jonasson and Callaghan, 1992). Quantitative data on root traits and architecture is one of the most significant variables considered when plants are evaluated for soil stabilization (Stokes et al., 2009). However data on root traits of alpine species remains scarce (Hu et al., 2013; Jonasson and Callaghan, 1992; Nagelmüller et al., 2016; Onipchenko 2014; Pohl et al., 2011; Zoller and Lenzin, 2006) which limits our understanding of the role these plants can play in root-soil interactions on the forefield.

Traditional techniques applied to examine the root system such as rhizotron or mini rhizotron, the use of paper pouches, synthetic soil media are all limited by the visual tracking of roots and/or creating an artificial environment that can lead to distorted/deceptive results. Destructive root phenotyping methods can also produce misleading results (Mooney et al., 2012) as they involve the separation of roots from the soil media meaning the relationship of the roots to the soil and to each other can no longer be observed (Pierrer et al., 2005). Additionally, repeated analysis on the same root system over time cannot be carried out e.g., dynamics of root growth or derivation of root demography (Koebernick et al., 2014).

Non-destructive imaging techniques such as Neutron Radiography, Magnetic Resonance Imaging (MRI) and X-ray Computed Tomography (X-ray CT) have been

effectively used in root phenotyping as they overcome the limitations of traditional techniques and able to provide results on intact root systems in undisturbed soil. Research involving modeling (e.g., Water Erosion Prediction Project (WEPP) or Chemicals, Runoff and Erosion from Agricultural Management Systems (CREAMS)) also benefits from the enhanced quality of numerical data on root traits provided by these state of the art techniques (Lobet et al., 2015; Tasser and Tappeiner, 2005).

X-ray CT has already been successfully employed in many studies focusing on plant roots (e.g., Aravena et al., 2011; Mooney et al., 2006; Pierret et al., 1999; Wantanabe et al., 1992) to obtain clear, 3D images of intact root systems in the soil without the paramagnetic (Materials that are attracted by an externally applied magnetic field and form internal, induced magnetic fields in the direction of the applied magnetic field. (Boundless, 2016)) impact on the image quality found in MRI (Mooney et al., 2012; Koebernick et al., 2014). Whilst the majority of X-ray CT studies have been carried out on agricultural species such as wheat (Jenneson et al., 1999; Gregory et al., 2003; Mooney et al., 2006), maize (Lontoc-Roy et al., 2006), soybean (Tollner et al., 1994), potato (Han et al., 2008) and tomato (Tracy et al., 2012), a few studies can be found on tree roots (Pierret et al., 1999; Kaestner et al., 2006; Paya et al., 2015) and grasses (Pfeifer et al., 2015). As yet, no research has been carried out on the root architecture of alpine species under natural soil conditions using the X-ray CT.

In the majority of these studies, sieved, pre-prepared low organic content soils were used as the plant growth matrix, as the greater amount of organic particles can make root differentiation from soil particles more difficult, hampering root segmentation (process of partitioning a digital image into multiple segments). Moreover, the

moisture distribution within undisturbed soil is more inconsistent which may also complicate the image segmentation process due to variations in image grayscale range of the roots under investigation (Pfeifer et al., 2015). While there have been a number of studies on the relationship between the natural soil matrix and the roots that permeate it, these studies have tended to focus on aspects of soil architecture rather than the architecture of the root (e.g., soil macropores, soil pore space) (e.g., Hu et al., 2016; Kuka et al., 2013).

The aim of the present study is to investigate and compare the root architecture and root traits of the ten most dominant pioneer plant species of the forefield of Lys Glacier (NW Italian Alps) in their natural soil system by producing accurate 3D images of their root system using X-ray CT. The value of the X-ray CT is verified by comparing the obtained results with other commonly employed techniques. Moreover, root tensile strength measurements will be made to understand the biomechanical role of the plant species on soil stabilisation. The retrieved information is discussed in the light of the potential future use of the studied species for slope soil reinforcement.

2. Materials and methods

2.1 Study site

Plant sampling was carried out on the recently deglaciated forefield of the Lys Glacier in the Aosta Valley (North West Italy). The glacial till was deposited in 2004

150 at an altitude of 2300 m above sea level on a bedrock of granitic gneiss and
151 paragneiss belonging to the Monte Rosa nappe (D'Amico et al., 2014). The climate
152 is alpine subatlantic with a mean annual rainfall of 1200 mm. The mean annual air
153 temperature is -1 °C (Mercalli, 2003) with a winter temperature below -4 °C on
154 average. The sampling site is south facing with a soil texture of loamy sand and an
155 udic moisture regime (Soil Survey Staff, 2010). The chemical properties of the soil at
156 the study site correspond to a slightly acidic soil (pH 5.8 - 6.7) with very low amounts
157 of total nitrogen (TN) and total organic carbon (TOC) (0.002-0.017 g kg^{-1} and 0.018-
158 0.217 g kg^{-1} respectively) with available phosphorus (P) of 1.3-4.7 mg g^{-1}. Pioneer
159 alpine plants, mostly graminoid and forb species colonize the site (e.g., *Epilobium*
160 *fleischeri* Hochst., *Linaria alpina* (L.) Mill., *Trisetum distichophyllum* (Vill.) P.
161 Beauve.), a detailed vegetation survey of the moraine can be found in D'Amico et al.
162 (2014).
163
164 ## 2.2 Sampling approach
165
166 The ten most common plant species of the forefield were selected. These were
167 sampled between August and September 2015; *E. fleischeri*, *T. distichophyllum*,
168 *Trifolium pallescens* Schreb., *Luzula spicata* (L.) DC., *Silene exscapa* All., *Minuartia*
169 *recurva* (All.) Schinz and Thell., *Festuca halleri* All. *Poa laxa* Haenke, *Salix helvetica*
170 Vill. and *Leucanthemopsis alpina* (L.) Heyw (Table1). A total of 60 soil columns, (i.e.
171 6 columns per species) were excavated. During sampling, special care was taken to
172 avoid individuals with any visible neighbouring plant effects (Gaudet and Keddy,
173 1988) and to keep plant size as equal as possible for all 60 samples. One sample
174 from each species was cored 10 samples in total) with their own PVC cylinder

(maximum sample height of 20 cm x diameter of 7.4 cm). After coring, the ten soil columns were carefully secured and placed in plastic bags and transported to the laboratory. In the laboratory the cored samples were placed in a climate chamber until the X-ray CT tests were undertaken. The climate chamber was set to provide conditions so as to delay root decay using a photoperiod of 14 hours, a relative humidity of 65 % and temperatures of 15 °C by day and 10 °C by night.

The remaining five replicates of each species (a total of 50) were excavated with a trowel. The 50 soil columns containing the root system of the individuals were placed in plastic bags, transported to the laboratory and stored at 3.5 °C until measurements were undertaken (Bast et al., 2015).

Table1.

Species	Common name	Life form	Succession	Family
Epilobium fleischeri Hochst.	Alpine willowherb	Forb	Early	Omagraceae
Trisetum distichophyllum (Vill.) P.Beauve.	Tufted hairgrass	Graminoid	Early	Poaceae
Trifolium pallescens Schreb.	Pale clover	Forb	Early	Fabaceae
Luzula spicata (L.) DC.	Spiked woodrush	Graminoid	Mid	Juncaceae
Silene exscapa All.	Moss campion	Forb	Mid	Caryophyllaceae
Minuartia recurva (All.) Schinz and Thell.	Recurved sandwort	Forb	Late	Caryophyllaceae
Festuca halleri All.	Haller's Fescue	Graminoid	Late	Poaceae
Poa laxa Haenke	Banff Bluegrass	Graminoid	Ubiquitous	Poaceae
Salix helvetica Vill.	Swiss willow	Dwarf shrub	Ubiquitous	Salicaceae
Leucanthemopsis alpina (L.) Heyw.	Alpine Moon Daisy	Forb	Ubiquitous	Asteraceae

2.3 Non-destructive root phenotyping

The cored samples from the PVC cylinder were scanned using a Phoenix V|TOME|X M 240 high resolution X-ray CT system (GE Sensing and Inspection Technologies, Wunstorf, Germany). The scanning parameters (Table 2) were optimized to allow balance between a large field of view and a high resolution. Due to the height of the cylinder (20 cm) two separate scans (upper and lower part of the sample) were

made to cover and image the entire sample. Each sub-scan was then reconstructed using DatosRec software (GE Sensing and Inspection Technologies, Wunstorf, Germany) and then manually combined in VG Studio MAX v2.2 (Volume Graphics GmbH, Heidelberg, Germany) and exported as a single 3D volumetric dataset. To distinguish the root system from the soil material image processing techniques were applied. Roots were segmented from the reconstructed CT data by using the region growing method (Gregory et al., 2003) in VG Studio MAX v2.2. Quantification of 3D root traits was undertaken using RooTrak software (Mairhofer et al., 2012). RooTrak was able to provide quantitative data on the root volume (total mass of the root system; mm^3), root area (root area in direct contact with the soil; mm^2), the root system's maximum vertical and horizontal length (mm) as well as the convex hull (the region of soil explored by the root system; mm^3) (Mairhofer et al., 2015).

Table 1 Scanning parameters for X-ray CT.

2.4 Destructive root phenotyping

Following X-ray CT scanning, the roots were extracted from the soil column by carefully cleaning the soil matrix from the roots with a water jet under a sieve mesh to retain remnants of roots that may come loose during the cleaning process. The washed roots were then placed into a 15 % ethanol solution and stored at 3.5 ºC. Then the root systems were scanned with a flatbed scanner (EPSON Expression 11000XL). The images from scanning had a 600 dpi resolution and were used for two dimensional image analysis. This was with the aim to compare the CT scanned results with the results of a, traditional technique (Paez-Garcia et al., 2015). Root

traits such as total root length, average root diameter, and the root system's maximum vertical and horizontal length were considered for analysis.

The remaining 50 plant samples (five replicates of each species were followed the same cleaning, storing and scanning method as before . All 2D scanned images were analyzed with the WinRHIZO 2013e and ImageJ software. The data collected on root traits were total root length, root length distribution (%) in different diameter classes, average root diameter, root length density, rooting depth and total plant height. Additionally plant height was measured according to the standardized measurement of plant functional traits (Pérez-Harguindeguy et al., 2013).

2.5 Root tensile strength

Root tensile strength tests were performed to determine root resistance to breaking under tension (Bischetti et al., 2005; Pohl et al., 2011). The complete root system, kept in a 15 % ethanol solution was first cut into individual root segments. Randomly selected undamaged roots with the widest available range of diameters were then selected for testing. Before testing, root diameter at three points of the root segment were measured with a digital caliper to obtain the average root diameter of the individual root sample. This is necessary as the exact position of root rupture is unknown before testing.

Root tensile strength were measured in the laboratory using an electromechanical universal testing machine, MTS Criterion, Model 43 (MTS Systems, Eden Prairie, MN, USA). Plant roots were secured between clamps at both ends. The clamps consist of two metal discs (washers) covered with drafting tape holding the roots in place. The speed reduction of the device was maintained at a steady 10 mm min^{-1} as

it was suggested in other studies (Bischetti et al., 2005; Bordoni et al., 2016; De Baets et al., 2008; Yang et al., 2016) and the tensile force was measured by a load cell (500N) connected to a computer to record the results. Roots broke when they could no longer resist tensile force. Measurement results were excluded from data analysis when root rupture occurred near the clamp. Measurement considered to be successful when the rupture occurred in the middle of the root section

2.6 Statistical analysis

In the present study comparative data analysis on root traits between the non-destructive and destructive technique was only respected when comparing the maximum vertical and horizontal length of the root system due to the lack of data available on very fine roots (< 0.5 mm) on the 3D images.

Results obtained from X-ray CT scanning (RooTrak) on the root system's maximum vertical and the maximum horizontal length were compared with results obtained from the destructive method (ImageJ) by applying Pearson's correlation test. Once the normality and homogeneity of variance were verified a one-way analysis of variance (ANOVA) was used to detect differences in the measured root properties (root length density, total root length, mean root diameter, rooting depth, root length distribution within diameter classes) and plant height among the studied species. In cases when significant differences were found between the groups, the Tukey post hoc test was run to detect where the differences occurred between the groups.

The relationship between root tensile strength and root diameter was evaluated by fitting a regression curve (power law equation). Analysis of covariance (ANCOVA) was performed to compare tensile strength results between the 10 studied species

and to take root diameter into consideration as a covariant. Both tensile strength and root diameter values were log transformed before the analysis. All assumptions were tested before carrying out ANCOVA (linearity, homogeneity and normality) . All statistical analysis was carried out using the statistical software SPSS Statistics 22 (IBM SPSS, 2013).

3. Results

3.1 Non-destructive root phenotyping

X-ray CT was successfully used to reveal the 3D root architecture of the studied 10 species. Tap roots and thicker lateral roots (diameter >0.5 mm) were identified in all cases while individual examples of thinner lateral roots (diameter < 0.5 mm) were only identified for *S. helvetica*, *P. laxa*, *L. spicata* and *F. halleri,* (diameters of 0.35, 0.35, 0.25 and 0.25 mm, respectively). Even though it was not possible to extract the entire root system, a visual representation of root–soil contact in the undisturbed position, orientation and elongation of the core root system was possible. It should be noted that due to the size limitation of the PVC cylinder and the difficulty of identifying root position when coring, the tap root and/or lateral roots were cut off by the edge of the cylinder therefore the max vertical and horizontal root length in the present study is approximate and should only be taken into consideration as part of data validation for RooTrak.

The maximum vertical and horizontal root length data obtained from the 3D images were underestimated by an average of 42% and overestimated by 26% respectively

when compared to measured data with ImageJ. The results from the Pearson's correlation tests between RooTrak and ImageJ showed a week positive correlation (r= 0.57, p=0.084) for maximum vertical root length (Figure 3a) and a very week negative correlation (r= -0.38, p=0.275) for the maximum horizontal root length (Figure 3b). Because the p-values are greater than the significance level of 0.05, there is inconclusive evidence about the significance of the association between the variables.

The highest root volume, root area and convex hull (Table 3) were all recorded for *T. pallescens* (1530 mm^3, 7752 mm^2, 505384 mm^3 respectively). The lowest root volume was recorded for *M. recurva* and *P. laxa* (144 and 150 mm^3 respectively) while the lowest value of root area (1146, 1547 and 1677 mm^2) and convex hull (24117, 45612, 60237 mm^3) was recorded for *S. helvetica, P. laxa* and *M. recurva* respectively. Results from *F. halleri* and *L. spicata* were excluded from the comparison as it was difficult to identify and segment the high number of fine (< 0.25 mm), overlapping roots and in many cases it was not possible at all. Therefore including the results of *F. halleri* and *L. spicata* would have caused misleading overall results.

Table 3. Values of root traits analyzed with RooTrak (volume, area, maximum vertical and horizontal length of the root system, convex hull), ImageJ (maximum

vertical and horizontal length of the root system) and WinRHIZO (total root length and average root diameter) of the X-ray CT scanned samples.

The highest total root length was recorded for *T. distichophyllum*, *L. spicata* and *S. exscapa* (192.7, 100.3 and 95.3 m respectively) and the lowest for *P. laxa* and *F. halleri* (10.5 and 20.7 m respectively). The rest of the species results fell between the values of 50.5 and 62.2 m (Table 3).

Average root diameter ranged between 0.16 and 0.31 mm. The lowest root diameters were recorded for *L. spicata* and *E. fleischeri* (0.16 mm and 0.17 mm respectively) and the highest for *P. laxa* and *T. pallescens* (0.31 mm and 0.30 mm respectively) (Table 3).

Figure 3 *a.,* Linear correlation between RooTrak and ImageJ data on the maximum vertical and *b.,* horizontal root length for the 10 studied alpine species.

The overall root architecture for each species displayed considerable variation (Figure 1 a-j). To determine and differentiate root system architecture between the species the root type classification established by Lichtenegger and Kutschera, (1991) was applied:

E. fleischeri showed a dominant pole root system with strong horizontal root spreading indicating the intense clonal growth of the plant. *T. pallescens* showed a cone shape and *S. exscapa* a wider cone shape upward extended root type. *S. helvetica* and *M. recurva* had a discoid shaped root system due to the shallow depth of rooting but large lateral spreading. *P. laxa*, *F. halleri* and *L. spicata* all showed a

cone shape downwards dilated root type while *L. alpine* had an umbrella shaped and *T. distichophyllum* a cylindrical shaped root type.

Figure1. Root architecture of the 10 studied pioneer alpine species detected by X-ray CT scanning. Scale bars: a., 35 mm, b., 25 mm, c., 40 mm, d., 15 mm, e., 10 mm, f., 15 mm, g., 15 mm, h., 30 mm, i., 45 mm, j., 20 mm.

Figure 2 *a.,* Image of the core root system *b.,* the core root system in relation to the soil matrix and *c.,* the washed entire root system of *T. pallescens*. Scale bar a., 45 mm b., 40 mm and c., the ruler uses cm.

The natural soil matrix showed a great variation in terms of soil structure among the cored samples. Figure 5 a-c shows examples of the structural diversity of the samples. The soil matrix in Figure 5 a., indicates a deposition of glacial till with little reorganization due to slope processes as Figure 5 b., and c., are fluvio-glacial and lake depositions with visible silt and sand layers.

Figure 5 Examples of the grayscale CT images of the soil matrices *a.,* glacial till with *T. distichophyllum b.,* and *c.,* fluvio-glacial and lake depositions.

3.2 Destructive root phenotyping

Root length density results varied greatly among the studied species (9.3–85 cm cm^{-3}). The lowest density was recorded for *E. fleisheri*, *M. recurva* and *T. pallescens*, with 9.3, 29 and 33 cm cm^{-3} respectively and the highest was recorded for *T.*

distichophyllum and *L. spicata* with 85 and 81 cm cm^{-3} respectively. There was significant difference found in root length density among the species ($F(9, 22) = 4.78$, $p < 0.001$). Post-hoc comparisons using the Tukey HSD test indicated that root length density differed significantly ($p < 0.05$) between *E. fleisheri* and *L. spicata*, *T. distichophyllum*, *S. helvetica* and *F. halleri* as well as between *M. recurva* and *L. spicata*. There was no statistically significant difference in root length density between the other species. However, the difference between *T. pallescens* and *L. spicata* showed a substantial trend toward significance ($p=0.078$) as well as between *M. recurva* and *T. distichophyllum* ($p=0.062$). Specifically, the results suggest that out of the ten studied species, only *E. fleisheri's* and *M. recurva*'s root system resulted in a significantly lower root length density when compared to the majority of the studied plants. It should be noted that in most but not all cases, higher root length density was found among the graminoid (*L. spicata, T. distichophyllum, F. halleri*) and the dwarf shrub (*S. helvetica*) species.

Total root length results (Table 4) showed no significant differences between the species ($F(9, 39) = 1.07$, $p=0.417$) even though the mean results showed moderate variability among them (75.3–368.5 m). The shortest length was recorded for *E. fleischeri*, and *S. exscapa*, with 75.3 and 106.2 m respectively and the highest for *L. alpina* and *S. helvetica* with 368.5 and 342.3 m respectively.

Table 4 Plant height (mm), rooting depth (mm) measured with ImageJ, total root length (m), mean root diameter (mm) and root length density (cm cm-3) of the 10 studied alpine species measured with WinRhizo.

393 Table 5 shows the root length distribution in different diameter classes (%). Eight out
394 of ten species had their highest root count (57-36 %) in the diameter class 0<L<=0.1
395 mm with the exception of *T. distichophyllum* and *S. helvetica* which had it at
396 0.1<L<=0.2 (41 %) and 0.2<L<=0.3 mm (37 %) respectively. *T. pallescens* and *S.*
397 *helvetica* also had roots larger than 2 mm in diameter as the other species rarely
398 exceeded 1 mm in diameter.
399
400 **Table 5** Root length distribution (%) of the 10 pioneer alpine plants in relation to
401 different diameter classes (mm).
402 Figure
403
404 The mean root diameter results (Table 3) also showed no significant differences
405 between the species (F (9, 22) =1.78, p=0.129) values. The results ranged between
406 0.21 mm and 0.47 mm. The lowest mean root diameter was recorded for *T.*
407 *distichophyllum* with 0.21 mm and the highest for *T. pallescens* with 0.47 mm.
408
409 Rooting depth results (Figure 6), determined by ImageJ showed considerable
410 variation among the species, ranging from 9 to 19.7 cm. The deepest penetrating
411 root system was recorded for *E. fleischeri* and the shallowest for *S. helvetica*. A one-
412 way ANOVA was used to compare the rooting depth results between the 10 species
413 which showed significant difference at F (9, 38) = 2.38, p <0.03. The Tukey HSD test
414 indicated that *E. fleischeri* had a significantly (p <0.05) longer rooting depth than *S.*
415 *helvetica* and *F. halleri*.
416 Plant height also varied between the species, ranging from 15 to 65 cm. The highest
417 plant height was recorded for *E. fleischeri* and the lowest for *M. recurva*. There was

significant differences found at F (9, 29) = 57.73, P< 0.000 between the studied species.

Figure 6 Plant height (cm) and rooting depth (cm) of the 10 studied alpine plant species.

3.3 Root tensile strength

There was a great variation in the tensile strength results among the studied species (Table 5). The highest mean tensile strength was found at the graminoid and shrub species ranging between 138-86 MPa and the lowest among the forbs ranging between 60-29 MPa. The results showed that graminoid species have comparable tensile strength results to the dwarf shrub *S. helvetica*. When the significant differences were tested between the studied species taken root diameter into consideration as a covariate the results showed significant differences between the studied species at F()=, p<0.

Tensile strength and the related root diameter values were plotted (Figure 7) to show the relationship between root tensile strength and root diameter which confirmed the power law relationship meaning that with increasing root diameter root tensile strength decreased.

Table 6 Life forms, the number of samples (n) tested, the range of root diameters (mm), root tensile strength (MPa) values, scale factor (α) rate of strength decrease (β) and the goodness of fit (R^2) of the 10 studied alpine species.

Table 7 ANOVA table with multiple comparisons of root tensile strength (MPa) between the studied plant species.

Figure 7 The relationship between root tensile strength (MPa) and root diameter (mm) for the 10 studied alpine species

4. Discussion

4.1 Non-destructive root phenotyping

The X-ray CT scanning has provided the first ever 3D images of the intact core root system of 10 different pioneer alpine plant species in their natural soil matrix. Visual information on the vertical and horizontal spreading as well as the rooting angle and branching of thicker roots in connection to the soil matrix were visible and could be important information when determining the significance of the root system on soil reinforcement in future studies (e.g. the resistance of the root system to uprooting or its protective role against shallow landsliding). During the use of X-ray CT several challenges and limitations were discovered; The following aspects made it difficult to decide on the scanning parameters: There was a limited amount (Stöckli and Bäumler, 1996; Pohl et al., 2011) or no data available on the root traits of the studied species prior to testing. They also had varying characteristics in terms of life form, family (Körner, 2003; Pignatti, 2003; Broglio and Poggio, 2008) and succession (Damico et al., 2014; Stöcklin and Bäumler, 1996) indicating different root

468 architecture and anatomy. Additionally they had never been subject to study with
469 current state of the art phenotyping techniques. The samples were cored from their
470 natural habitat in a heterogenic soil matrix and the soil absorbed a high level of the
471 X-rays resulting in prohibitively long scans to achieve the necessary beam
472 penetration. The tracking of individual roots during segmentation was extremely
473 difficult as the heterogenic soil matrix made it difficult to differentiate roots from other
474 organic particles in the soil (Figure 4 a, b, and c). Additionally the root system
475 contained vast amounts of overlapping roots and neighbouring plant roots were
476 invariably cored together with the test sample even when, from the surface, samples
477 appeared free from any neighbouring plant effects.
478 Roots with a diameter >0.5 mm are visible on the 3D images, these thicker roots
479 allow us to estimate the location of thinner roots (Stokes et al., 2009). Not being able
480 to detect the thinner roots on the present 3D images was not due to the limitations of
481 the X-ray CT technology, rather the issue of resolution, sample size and the
482 heterogenic soil matrix. In general, in homogeneous background the minimum
483 resolution should be set twice as high as the cored sample is long in millimeters and
484 set even higher if the background is heterogenic (Kaestner et al., 2006). A higher
485 resolution setting however would have resulted in a prohibitively prolonged scanning
486 and segmenting time. The method suggested by Kaestner et al. (2006) was
487 successful at detecting roots with a diameter <0.5 mm in homogeneous background
488 however roots in heterogeneous soil matrix (Figure 4 a-c) remained challenging.
489 Cored samples of reduced length and diameter may have allowed for the detection
490 and segmentation of the finer roots within the system but the compromise would be
491 the smaller PVC cylinders would not have been suitable for sampling the species
492 from the field without causing damage i.e. preventing disturbed soil conditions within

493 the sample. A factor to possibly bear in mind for future work conducted on alpine
494 species with fine root systems would be to take two sets of cores when assessing
495 the different scales in root architecture.
496 Interestingly, although it was not possible to segment using the available software;
497 many of the fine roots were often visible to the naked eye when manually scrolling
498 through the greyscale images providing a unique insight into the complexity of these
499 alpine species.
500
501
502
503 4.2. Analysis of root architecture and root traits
504 *S. exscapa* and *T. pallescens* both have a dominant tap root morphology with a large
505 number of tillers. Their tap root and thicker lateral roots are often found growing
506 through cracks in the bedrock thereby anchoring the plant and stabilizing the soil
507 from shallow landsliding. The number of lateral roots and the diversity of their
508 branching angles resulting in a larger shear zone indicate an increased soil stability
509 (Abe and Ziemer, 1991). Both *S. exscapa* and *T. pallescens* have dense, fine root
510 networks that can play an important role in reducing soil erosion. Root nodules are
511 clearly visible on the roots of *T. pallescens* reflecting the existing association the
512 plant has with symbiotic nitrogen-fixing bacteria (Holzmann and Haselwandter,
513 1988).
514 *S. helvetica* also has a dominant taproot morphology with the potential of growing
515 through cracks in the bedrock though it has a shallower rooting depth than *S.*
516 *exscapa* or *T. pallescens*. *S. helvetica* has a large lateral spread in the upper soil

517 layer with a dense fine root network which can provide increased support in soil
518 erosion control and horizontal anchoring.
519 Due to the uniform length of the umbrella shaped root system of *L. alpina* it can be
520 easily uprooted (cit), therefore, its potential as soil reinforcement is greatly limited
521 although it is capable of trapping a significant amount of soil due to its dense fine
522 root network (Hudek et al., 2017) and reducing soil erosion.
523 The dominant pole type of root system of *E. fleischeri* showed the greatest rooting
524 depth with intensive rhizome spreading. The main feature of the plant's strategy is
525 rapid colonization of open space through wide lateral clonal spreading (Stöckli and
526 Bäumler, 1996) which is a typical strategy for early successional plants such as
527 *Hieracium staticifolium* All.*, Achillea moschata* (Wulfen) or *Cerastium pedunculatum*
528 Gaudin (Stöckli and Bäumler, 1996). Its root system does not have notable
529 anchoring properties, its survival strategy relies on an elaborate network of rhizome
530 spreading, widely spaced ramets and rapid colonization (Alpandino, 2011). In this
531 way the plant is able to quickly overcome diverse mass wasting processes.
532 Additionally its short and fragile fine root (<1mm) network is unclearly able to provide
533 additional soil stabilization (Bischetti et al., 2009) even though plant biomass and
534 allometry are stated being a significant element when plants are evaluated for soil-
535 root reinforcement (Gonzalez-Ollauri and Mickovski, 2016). In general the function of
536 these roots is limited to water and nutrient uptake to support plant growth (Stokes et
537 al., 2009; Tasser and Tappeiner, 2005).
538 *T. distichofillum* also uses horizontal spreading through clonal growth as a strategy
539 for rapid colonization but with shorter distance between ramets (Alpandino, 2011). It
540 also has a dense lateral root system with moderate rooting depth and a high
541 percentage of fine and very fine roots throughout the entire root system. This can

make the plant more resilient to uprooting and at the same time, through the elaborate network of rhizome spreading, able to overcome diverse mass wasting processes (Körner, 2003). Its dense fine and very fine roots trap soil providing erosion control. *P. laxa* is a plant with clumped clonal growth form with short distance between ramets. *F. halleri* and *L. spicata* both form compact tussocks with a dense fibrous root system. This phalanx type of clonal growth results in a slow horizontal spreading (Alpandino, 2011). These types of root morphology can make the plants extremely resilient to uprooting and a potentially effective plant in erosion control.

The root architecture of the species showed a wide range of root types dictated by genetic characteristics (Gray and Sotir, 1996) and environmental factors e.g., nutrient availability or soil temperature (Nagelmüller et al., 2016; Khan et al., 2016). Root plasticity too has effects on root architecture, it is essential in coping with and overcoming stress (Bardgett et al., 2014; Poorter et al., 2012; Stöcklin and Bäumler, 1996) as well as strengthening the resilience of pioneer species to the harsh environmental conditions.

Even though *E. fleischeri* had a significantly higher rooting depth compared to the other species, in general, rooting depth was uniformly shallow which is in line with previous findings (Lichtenegger, 1996; Jonasson and Callaghan, 1992; Pohl et al., 2011) on alpine species. This is influenced by two main controlling environmental factors; soil temperature and water availability (Lichtenegger, 1996; Körner, 2003). Alpine vegetation in general have a shallower rooting system than species from lowlands as at high altitudes with increasing soil depth, soil temperature and water fluctuations decrease at a higher rate than in the lowlands (Lichtenegger, 1996). This also can reflect on root distribution within the different soil horizons, indicating that

566 the high root density in the upper soil layer quickly decreases with increasing soil
567 depth (Lichtenegger, 1996).
568 Root length density has a great influence on soil stability (Bardgett et al., 2014;
569 Stokes et al., 2009) by altering the hydrological properties of the soil and increasing
570 the resistance of the roots for disruptive forces. All studied species had a large
571 amount of fine and very fine roots which is common in alpine species (Körner, 2003;
572 Pohl et al., 2011). In general, fine and very fine roots have a rapid turnover supplying
573 a large amount of carbon to the soil and increasing the organic content of the soil.
574 Together with the physical and chemical contribution they gradually increase the
575 aggregate stability of the soil which reduces the susceptibility of the soil to erosion
576 processes (Pohl et al., 2011; Hudek et al., 2017). Additionally, both live and dead
577 roots provide potential preferential flow paths in hillslopes, securing the stability of
578 the soil by reducing pore water pressure (Ghestem et al., 2011). On the other hand,
579 bypass flow can lead to perched water tables, saturating the soil that can develop
580 positive pore-water pressure that could trigger landslides (Ghestem et al., 2011).
581 Glacier forefields are nutrient limited soils; fine and very fine roots (< 0.5 mm)
582 however, provide strong symbiotic links between the plant and the fungus systems
583 and it has been proven that mycorrhizal fungi increases the water and nutrient
584 uptake of the plant (Smith and Read, 2008) and promotes root growth (Ola et al.,
585 2015) which also influences RLD (Bast et al., 2014; Graf and Frei 2013; Tisdall,
586 1991). The dense fine root system of the studied species is also able to mechanically
587 bind the soil particles thereby contributing to increased soil stabilization (Pohl et al.,
588 2011; Norris et al., 2008).
589 In the present study the total root length values showed non-significant difference
590 between the species and life forms while the highest values were recorded among

591 the graminoid species as was with the work of Pohl et al. (2011) though in the
592 present study the measured values greatly exceed those of Pohl et al. (2011). This
593 can be attributed to the fact that at the sampling site of Pohl et al., (2011) sampling
594 was carried out on managed ski slopes where soil compaction inhibits root growth
595 (Nagel et al., 2012; Pfeifer et al., 2014) while in the case of our study on the recently
596 deglaciated forefield, sampling was performed on a site relatively free from human
597 interference and soil compaction was not an inhibiting factor for root growth.
598 Under natural conditions species grow together creating a complex underground root
599 network/structure due to the diversity of root types, enlarging the protective role of
600 plants on soil stabilization at different levels and soil layers (Pohl et al., 2009;
601 Reubens et al., 2007). Plant richness should therefore be encouraged when plants
602 are considered for soil conservation purposes such as land reclamation.
603
604 4.3. Root tensile strength
605
606 The tensile strength results of the present study were 3-7 times higher than those
607 found in literature data on the same alpine species (*L. spicata, L.alpina*) (Pohl et al.,
608 2011) and other alpine and arctic graminoid and forb species (Pohl et al., 2011,
609 Jonasson and Callaghan, 1992). Root tensile strength is mainly effected by the
610 genetic properties of the plant (Gray and Sotir, 1996) while additional factors such as
611 age (Reubens et al, 2007), ecological conditions and management
612 practices(Bischetti et al., 2009) can result in varying tensile strength values for the
613 same species. Gonzallez-Ollauri et al. (2017) highlighted that root tensile strength
614 can vary with changes in root moisture content which closely links to soil moisture
615 content (i.e. dry roots have a lower level of tensile strength compare to roots with

optimum root moisture). Root diameter has direct influence on root tensile strength as root tensile strength is calculated by the ratio between the breaking force (N) and the root cross section area (mm^2) which depends on root diameter (Bischetti et al., 2016). In general, fine and medium size roots (in diameter 0.01-10.00 mm) have higher values of tensile strength compared to roots with a larger diameter (> 10.00 mm). Larger sized roots act primarily as individual anchors mobilising only a small amount of their tensile strength before slipping through the soil (Bischetti et al., 2005). However, fine and medium sized roots can mobilize their entire tensile strength and due to their higher surface area, have superior resistance to uprooting (Gray and Sotir, 1996). In the present study the diameter of the tested roots ranged between 0.03 mm and 1.66 mm, these values are smaller than what is found in the literature data which can be one of the explanation for the considerably higher tensile strength results. Additionally the samples in Pohl et al. (2011) were collected from a managed ski slope which confirms results observed by Bischett et al. (2009) that ecological conditions and management can alter tensile strength.

It was possible to demonstrate the significant relationship between tensile strength and root diameter the plotted tensile strength results can demonstrate the power law relationship and can be used to make comparisons between species.

5. Conclusions

This study aimed to provide information on root morphology and root traits on pioneer alpine species from a recently deglaciated site in the Italian Alps with the view to determine the plants' efficiency in soil stabilization. To provide unique visual 3D data on the root architecture of a wide variety of alpine pioneer species under

intact natural soil conditions, we applied a state of the art non-destructive plant phenotyping technique, X-ray CT. This is the first study that uses the X-ray CT technique to image the root system of alpine plants undisturbed in their natural alpine soil matrix.

Results showed great variation in global root architecture between the studied species. X-ray CT could successfully identify roots >0.25, 0.35 mm in diameter at the resolution used for scanning. With complementary use of destructive phenotyping techniques, quantitative data on root traits and the plants biomechanical characteristic allowed us to determine species' efficiency in soil stabilization. The high tensile strength results of graminoid and the dwarf shrub species combined with a dense elaborate root morphology, provide many anchoring points and enhanced plant resilience to solifluction in a periglacial environment. While forbs longer, anchoring root system with lower but comparable tensile strength to the garminoid and dwarf shrub species, could advocate their suitability as protection against shallow landsliding. With the exception of one or two species (*E. fleischeri, M. recurva*) all studied plants play an important role in soil erosion control due to their dense elaborate fine and very fine root system.

Acknowledgements

This research was enabled by the Transnational Access capacities of the European Plant Phenotyping Network (EPPN, grant agreement no. 284443) funded by the FP7 Research Infrastructures Programme of the European Union. As well as receiving funding from the European Union's Horizon 2020 research and innovation programme under the Marie Skłodowska-Curie grant agreement No 609402 - 2020

researchers: Train to Move (T2M). The Hounsfield Facility received funding from European Research Council (Futureroots Project), Biotechnology and Biological Sciences Research Council of the United Kingdom and The Wolfson Foundation.

The authors wish to thank Alessio Cislaghi, Enricho Chiaradia and Gian Battista Bischetti for the access to and support with the tensile testing machine and Michele Lonati for his help on the identification of graminoid species.

References

Abe, K., Ziemer, R.R., 1991. Effect of tree roots on a shear zone: modeling reinforced shear stress. Canadian Journal of Forest Research 21, 1012-1019.

Alpandino, 2011. Alpandino by Institute of Botany, University of Basel, Switzerland. https://www.alpandino.org

Aravena, J.E., Berli, M., Ghezzehei, T.A., Tyler, S.W., 2011. Effects of root-induced compaction on rhizosphere hydraulic properties X-ray microtomography imaging and numerical simulations. EnvSci & Tech, 45, 425–431.

Bardgett, R.D., Mommer, L., De Vries, F.T., 2014. Going underground: root traits as drivers of ecosystem processes. Trends in Ecology and Evolution, 29, 12, 692-699.

Bast, A., Wilcke, W., Graf, F., Lüscher, P., Gärtner, H., 2015. A simplified and rapid technique to determine an aggregate stability coefficient in coarse-grained soils. Catena, 127, 170-176.

Bischetti, G.B., Bassanelli, C., Chiaradia, E.A., Minotta, G., Vergani, C., 2016. The effect of gap openings on soil reinforcement in two conifer stands in northern Italy. Forest Ecology and Management, 359, 286–299.

691 Bischetti, G.B., Chiaradia, E.A., Epis, T., Morlotti, E., 2009. Root cohesion of forest
692 species in Italian Alps. Plant and Soil, 324, 71-89.
693 Bischetti, G.B., Chiaradia, E.A., Simonato, T., Speziali, B., Vitali, B., Vullo, P., Zocco,
694 A., 2005. Root strength and root area ratio of forest species in Lombardy
695 (Northern Italy). Plant and Soil, 278, 11–22
696 Bordoni, M., Meisina, C., Vercesi, A., Bischetti, G.B., Chiaradia, E.A., Vergani, C.,
697 Chersich, S., Valentino, R., Bittelli, M., Comolli, R., Persichillo,
698 M.G., Cislaghi, A., 2016. Quantifying the contribution of grapevine roots to
699 soil mechanical reinforcement in an area susceptible to shallow landslides.
700 Soil and Tillage, 163, pp. 195-206.
701 Boundless. “Diamagnetism and Paramagnetism.” *Boundless Chemistry* Boundless,
702 08 Aug. 2016. Retrieved 03 Mar. 2017.
703 https://www.boundless.com/chemistry/textbooks/boundless-chemistry-
704 textbook/periodic-properties-8/electron-configuration-68/diamagnetism-and-
705 paramagnetism-320-10520/
706 Bradley, J.A., Singarayer, J.S., Anesio, A.M., 2014. Microbial community dynamics in
707 the forefield of glaciers. Peoc. R. Soc.B 281: 20140882.
708
709 Broglio, M., Bovio, M., Poggio, L., 2008. Guida alla flora della Valle d'Aosta.
710 D'Amico, M.E., Freppaz, M., Filippa, G., Zanini, E., 2014. Vegetation influence on
711 soil formation rate in a proglacial chronosequence (Lys Glacier, NW Italian
712 Alps).CATENA, 113, 122-137.
713 Gaudet, C.L., Keddy, P.A., 1988. A comparative approach to predicting competitive
714 ability from plant traits. Nature, 334, 242–3
715 Ghestem, M., Sidle, R.C., Stokes, A., 2011. The influence of plant root system on
716 subsurface flow: Implications for slope stability. BioScience, 61, 869-879.

717 Gonzalez-Ollauri, A., Mickovski, S.B., 2016. Using the root spread information of
718 pioneer plants to quantify their mitigation potential against shallow landslides
719 and erosion in temperate humid climates. Ecological Engineering, 95, 302-
720 315.
721 Gonzalez-Ollauri, A., Mickovski, S.B., 2017. Plant-soil reinforcement response under
722 different soil hydrological regimes. Geoderma, 285, 141-150.
723 Gregory, P.J., Hutchinson, D.J., Read, D.B., Jenneson, P.M., Gilboy, W.B., Morton,
724 E.J., 2003. Non-invasive imaging of roots with high resolution X-Ray micro-
725 tomography. Plant Soil, 255, 351–359.
726 Graf, F., Frei, M., 2013. Soil aggregate stability related to soil density, root length,
727 and mycorrhiza using site-specific *Alnus ncana* and *Melanogaster variegatus*s
728 l.. Ecological Engineering, 57, 314-323.
729 Grey, D.H., Sotir, R.B., 1996.Biotechnical and soil bioengineering slope stabilization.
730 In: A practical guide for erosion control. Willey, John & Sons, New York, pp. 1-
731 105.
732 Han, L., Dutilleul, P., Prasher, S.O., Beaulieu, C., Smith, D.L., 2008. Assessment of
733 common scab-induced pathogen effects onpotato underground organs via
734 computed tomography scanning. Phytopathology, 98, 1118–1125.
735 Holzmann, H., Haselwandter, K., 1988. Contribution of nitrogen fixation to nitrogen
736 nutrition in an alpine sedge community (Caricetum curvulae). Oecologia, 76,
737 298-302. doi: 10.1007/BF00379967
738 Hu, X., Brierley, G., Zhu, H., Li, G., Fu, J., Mao, X., Yu, Q., Qiao, N., 2013. An
739 exploratory analysis of vegetation strategies to reduce shallow landslide activity
740 on loess hillslopes, Northeast Qinghai-Tibet Plateau, China. J. Mt. Sci., 10,
741 668–686.

742 Hu, X., Li, Z.C., Li, X.Y., Liu, L.Y., 2016. Quantification of soil macropores under
743 alpine vegetation using computed tomography in the Qinghai Lake Watershed,
744 NE Qinghai–Tibet Plateau. Geoderma, 264,244-251.
745 Hudek, C., Stanchi, S., D'Amico, M., Freppaz, M., (submitted) Quantifying the
746 contribution of the root system of alpine vegetation in the soil aggregate stability
747 of moraine.
748 IBM Corp. Released 2013. IBM SPSS Statistics for Windows, Version 22.0. Armonk,
749 NY: IBM Corp.
750 Jenneson, P.M., Gilboy, W.B., Morton, E.J., Luggar, R.D., Gregory, P.J., Hutchinson,
751 D., 1999. Optimisation of X-ray microtomography for the in situ study of the
752 development of plant roots. 1999 Ieee Nuclear Science Symposium
753 Conference Record, 1–3, 429–432.
754 Jonasson, S., and Callaghan, T.V., 1992. Root Mechanical Properties Related to
755 Disturbed and Stressed Habitats in the Arctic. The New Phytologist 122, 179-
756 186.
757 Jones, G.A. and Henry, G.H.R., 2003. Primary plant succession on recently
758 deglaciated terrain in the Canadian High Arctic. Journal of Biogeography, 30,
759 277–296. doi:10.1046/j.1365-2699.2003.00818.x
760 Kaestner, A., Schneebeli, M., Graf, F., 2006. Visualizing three-dimensional root
761 networks using computed tomography. Geoderma, 136, 459–469.
762 Khan, M.A., Gemenet, D.C., Villordon, A., 2016. Root System Architecture and
763 Abiotic Stress Tolerance: Current Knowledge in Root and Tuber Crops. Front.
764 Plant Sci., 7, Article 1584.
765 Koebernick, N., Weller, U., Huber, K., Schlüter, S., Vogel, H.J., Jahn, R.,
766 Vereecken,H., Vetterlein, D., 2014. *In situ* visualization and quantification of

767 three-dimensional root system architecture and growth using x-ray computed
768 tomography. Vadose Zone, 13, 1-10.
769 Körner, C., 2003. Alpine plant life Functional plant ecology of high mountain
770 ecosystems. Springer-Verlag Berlin.
771 Kuka, K., Illerhaus, B., C.A., Fox, Joschko, M., 2013. X-ray Computed
772 Microtomography for the Study of the Soil–Root Relationship in Grassland
773 Soils. Vadose Zone Journal, 12, 1-10.
774 Lazzaro, A., Franchini, A.G., Brankatschk, R., Zeyer, J., 2010. Pioneer communities
775 in the forefields of retreating glaciers: how microbes adapt to a challenging
776 environment. In: Current Research, Technology and Education Topics in
777 Applied Microbiology and Microbial Biotechnology (Edi.Mendes-Villas, A.)
778 Formatex, Badajoz, Spain.
779 Lichtenegger, E., 1996. Root distribution in some alpine plants. Acta Phytogeogr.
780 Suec., 81, 76-82.
781 Lichtenegger, E., and Kutschera-Nitter, L., 1991. Spatial root types. In Edited by
782 McMichael, B.L., and Persson, H. Development in agricultural and managed
783 forests ecology 24. Plant roots and their environment. Proceedings of an ISRR
784 symposium Elsevier Science Publisher B.V. Amsterdam, Netherlands.
785 Lobet, G., Pound, M.P., Diener, J., Pradal, C., Drayer, X., Godin, C., Javaux, M.,
786 Leitner, D., Maunier, F., Nancy, P., Pridmore, T.P., Schnepf, A., 2015. Root
787 system markup language: toward a unified root architecture description
788 language. Plant Physiology, 167, 617-627.
789 Lontoc-Roy, M., Dutilleul, P., Prasher, S.O., Han, L., Brouillet, T., Smith, D.L., 2006.
790 Advances in the acquisition and analysis of CT scan data to isolate a crop root

system from the soil medium and quantify root system complexity in 3-Dspace. Geoderma, 137, 231–241.

Mairhofer, S., Sturrock, C., Wells, D.M., Bennett, M.J., Mooney, S.J., Pridmore, T.P., 2015. On the evaluation of methods for the recovery of plant root systems from X-ray computed tomography images. Functional Plant Biology, 42, 460–470.

Mairhofer, S., Zappala, S., Tracy, S.R., Sturrock, C., Bennett, M., Mooney, S.J., Pridmore, T., 2012. RooTrak: Automated Recovery of Three-Dimensional Plant Root Architecture in Soil from X-Ray Microcomputed Tomography Images Using Visual Tracking. Plant Physiology, 158, 561–569.

Massaccesi, L., Benucci, G.M.N., Gigliotti, G., Cocco, S., Corti, G., Agnelli, A., 2015. Rhizosphere effect of three plant species of environment under periglacial conditions (Majella massif, central Italy). Soil Biology and Biochemistry, 89,184-195.

Matthews, J.A., 1999. Disturbance regimes and ecosystem response on recently-deglaciated terrain. In Ecosystems of Disturbed Ground, Walker LR (ed.). Elsevier: Amsterdam; 17–37.

Mercalli, L., 2003.Atlanteclimaticdella Valle d'Aosta. Societa Meteorologica Italia, Torino 405.

Mooney, S.J., Morris, C., Berry, P.M., 2006. Visualization and quantification of the effects of cereal root lodging on three-dimensional soil macrostructure using X-ray Computed Tomography. Soil Sci, 171, 706–718.

Mooney, S.J., Pridmore, T.P., Helliwell, J., Bennett, M.J., 2012. Developing X-ray Computed Tomography to non-invasively image 3-D root systems architecture in soil. Plant Soil, 352, 1-22.

816 Nagel, K.A., Putz, A., Gilmer, F., Heinz, K., Fischbach, A., Pfeifer, J., Faget, M.,
817 Blossfeld, S., Ernst, M., Dimaki, C., Kastenholz, B., Kleinert, A.K., Galinski, A.,
818 Scharr, H., Fiorani, F., Schurr, U., 2012. GROWSCREEN-Rhizo is a novel
819 phenotyping robot enabling simultaneous measurements of root and shoot
820 growth for plants grown in soil-filled rhizotrons. Functional Plant Biology, 39,
821 891-904. http://dx.doi.org/10.1071/FP12023
822 Nagelmüller, S., Hiltbrunner, E., Körner, C., 2016. Critically low soil temperatures for
823 root growth and root morphology in three alpine plant species. Alp Botany
824 126, 11–21.
825 Norris, J.E., Stokes, A., Mickovski, S.B., Cammeraat, E., Van Beek, R., Nicoll, B.C.,
826 Achim, A., 2008. Slope stability and erosion control: ecotechnological
827 solutions. Springer, Dordrecht.
828 Ola, A., Dodd, I.C., Quinton, J.N., 2015. Can we manipulate root system architecture
829 to control soil erosion? SOIL, 1, 603-612.
830 Onipchenko, V.G., Kipkeev, A.M., Makarov, M.I., Kozhevnikova, A.D., Ivanov, V.B.,
831 Soudzilovskaia, N.A., Tekeev, D.K., Salpagarova, F.S., Werger, M.J.A.,
832 Cornelissen, J.H.C., 2014. Digging deep to open the white black box of snow
833 root phenology. Ecol Res, 29, 529–534.
834 Paez-Garcia, A., Motes, C.M., Scheible, W.-R., Chen, R., Blancaflor, E.B., Monteros,
835 M.J., 2015. Root Traits and Phenotyping Strategies for Plant
836 Improvement. Plants, 4, 334–355.
837 Paya, A.M., Silverberg, J., Padgett, J., Bauerle, T.L., 2015. X-ray computed
838 tomography uncovers root-root interactions: quantifying spatial relationships
839 between interacting root systems in three dimensions. Frontiers in Plant
840 Science, 6, 274.

841 Pérez-Harguindeguy, N., Díaz, S., Garnier, E., Lavorel, S., Poorter, H.,
842 Jaureguiberry, P., Bret-Harte, M.S., Cornwell, W.K., Craine, J.M., Gurvich,
843 D.E., Urcelay, C., Veneklaas, E.J., Reich, P.B., Poorter, L., Wright, I.J., Ray,
844 P., Enrico, L., Pausas, J.G., de Vos, A.C., Buchmann, N., Funes, G., Quétier,
845 F., Hodgson, J.G., Thompson, K., Morgan, H.D., ter Steege, H., van der
846 Heijden, M.G.A., Sack, L., Blonder, B., Poschlod, P., Vaieretti, M.V., Conti, G.,
847 Staver, A.C., Aquino S., Cornelissen, J.H.C., 2013. New handbook for
848 standardised measurement of plant functional traits worldwide. Australian
849 Journal of Botany, 61, 167–234.
850 Pierret, J.S., Prasher, S.O., Kantzas, A., Langford, C., 1999. Three-dimensional
851 quantification of macropore networks in undisturbed soil cores. Soil Sci. Soc.
852 Am. J, 63, 1530–1543.
853 Pierret, A., Moran, C., Doussan, C., 2005. Conventional detection methodology is
854 limiting our ability to understand the roles and functions of fine roots. New
855 Phytol, 166, 967–980.
856 Pignatti, S., 2003. Flora D'Italia. Vol.3. Edagricole S.r.l., Bologna.
857 Pfeifer, J., Kirchgessner, N., Colombi, T., Walter, A., 2015. Rapid phenotyping of
858 crop root systems in undisturbed field soil using X-ray computed tomography.
859 Plant Methods, 11, 41.
860 Pfeifer, J., Faget, M., Walter, A., Blossfeld, S., Fiorani, F., Schurr, U., Nagel, K.A.,
861 2014. Spring barley shows dynamic compensatory root and shoot growth
862 responses when exposed to localised soil compaction and fertilisation.
863 Functional Plant Biology,41, 581-597.
864 Pohl, M., Alig, D., Körner, C., Rixen, C., 2009. Higher plant diversity enhances soil
865 stability in disturbed alpine ecosystems. Plant Soil, 324, 91–102.

866 Pohl, M., Stroude, R., Buttler, A., Rixen, C., 2011. Functional traits and root
867 morphology of alpine plants. Annals of Botany, 108, 537–545,
868 doi:10.1093/aob/mcr169
869 Poorter, H., Niklas, K.J., Reich, P.B., Oleksyn, J., Poot, P., Mommer, L., 2012.
870 Biomass allocation to leaves, stems and roots: meta-analyses of interspecific
871 variation and environmental control. New Phytologist. 193, 30-50.
872 Reubens, B., Poesen, J., Danjon, F., Geudens, G., Muys, B., 2007. The role of fine
873 and coarse roots in shallow slope stability and soil erosion control with a focus
874 on root system architecture: a review. Trees, 21, 385–402.
875 Robbins, J.A., Matthews, J.A., 2009. Pioneer vegetation on glacier forefields in
876 southern Norway: emerging communities? Journal of Vegetation Science, 20,
877 889-902.
878 Sati, S.P., Sundriyal, Y.P., 2007. Role of some species in slope instability.
879 Himalayan Geol., 28, 75-78.
880 Smith, S.E., Read, D.J., 2008. Mycorrhizal Symbiosis. Academic Press, Cambridge.
881 Soil Survay Staff, 2010. Keys to soil Taxonomy. United States Department of
882 Agriculture, Eleventh edition. Natural Resources Conservation Services.
883 Stokes, A., Atger, C., Bengough, A.G., Fourcaud, T., Sidle, R.C., 2009. Desirable
884 plant root traits for protecting natural and engineered slopes against landslides.
885 Plant Soil, 324, 1-30.
886 Stöcklin, J., Bäumler, E., 1996. Seed rain, seedling establishment and clonal growth
887 strategies on a glacier foreland. Journal of Vegetation Science., 9, 45-56.
888 Stöcklin, J., Kuss, P., Pluess, A.R., 2009. Genetic diversity, phenotypic variation and
889 local adaptation in the alpine landscape: case studies with alpine plant
890 species. Bot.Helv.119, 125-133.

Tasser, E., Tappeiner, U., 2005. New model to predict rooting in diverse plant community compositions. Ecological Modelling, 185, 195-211.

Tisdall, J.M., 1991. Fungal hyphae and structural stability of soil. Australian Journal of Soil Research, 29, 729-743.

Tollner, E.W., Rasmseur, E.L., Murphy, C., 1994.Techniquesand approaches for documenting plant root development with X-ray computed tomography. In Tomography of soil water-root processes. Edited by Anderson, S.H., and Hopmans, J.W., SSSA Special Publication, 36, Madison,Wis. 115–133.

Tracy, S.R., Black, C.R., Roberts, J.A., Sturrock, C., Mairhofer, S., Craigon, J., Mooney, S.J., 2012. Quantifying the impact of soil compaction on root system architecture in tomato (Solanum lycopersicum) by X-ray micro-computed tomography. Ann. Bot., 110, 511-519.

Wantanabe, K., Mandang, T., Tojo, S., Ai, F., Huang, B.K., 1992. Non-destructive root-zone analysis with X-ray CT scanner. Paper 923018. American Society of Agricultural Engineers. St Joseph, MI, USA

Yang, Y., Chen, L., Li, N., & Zhang, Q., 2016. Effect of Root Moisture Content and Diameter on Root Tensile Properties. *PLoS ONE*, *11*, e0151791.

Zoller, H., and Lenzin, H., 2006. Composed cushions and coexistence with neighbouring species promoting the persistence of *Eritrichium nanum* in high alpine vegetation. Bot. Helv., 116, 31–40.

Table and Figure Captions

Table 1

Table 2 Scanning parameters for X-ray CT.

Table 3 Values of root traits analyzed with RooTrak (volume, area, maximum vertical and horizontal length of the root system, convex hull), ImageJ (maximum vertical and horizontal length of the root system) and WinRHIZO (total root length and average root diameter) of the X-ray CT scanned samples.

Table 4 Plant height (mm), rooting depth (mm) measured with ImageJ, total root length (m), mean root diameter (mm) and root length density (cm cm^{-3}) of the 10 studied alpine species measured with WinRHIZO.

Table 5 Root length distribution (%) of the 10 pioneer alpine plants in relation to different diameter classes (mm).

Table 6 Life forms, the number of samples (n) tested, the range of root diameters (mm), root tensile strength (MPa) values, scale factor (α) rate of strength decrease (β) and the goodness of fit (R^2) of the 10 studied alpine species.

Table 7 ANOVA table with multiple comparisons of root tensile strength (MPa) between the studied plant species.

Figure1 a - j Root architecture of the 10 studied pioneer alpine species detected by X-ray CT scanning. a., *E. fleischeri*; b., *F. halleri*; c., *L. alpine*; d., *L. spicata*; e., *M. recurva*; f., *P. laxa*; g., *S. helvetica*; h., *S. exscapa*; i., *T. pallescens*; j., *T. distichophyllum*; Scale bars: a., 35 mm, b., 25 mm, c., 40 mm, d., 15 mm, e., 10 mm, f., 15 mm, g., 15 mm, h., 30 mm, i., 45 mm, j., 20 mm.

Figure 2 *a.,* Image of the core root system *b.,* the core root system in relation to the soil matrix and *c.,* the washed entire root system of *Trifolium pallescens*. Scale bar a., 45 mm b., 40 mm and c., the ruler uses cm.

Figure 3 *a.,* Linear correlation between RooTrak and ImageJ data on the maximum vertical and *b.,* horizontal root length for the 10 studied alpine species.

Figure 4

Figure 5 Examples of the grayscale CT images of the soil matrices *a.,* glacial till with *T. distichophyllum b.,* and *c.,* fluvio-glacial and lake depositions.

Figure 6 Plant height (cm) and rooting depth (cm) of the 10 studied alpine plant species.

Figure 7 The relationship between root tensile strength (MPa) and root diameter (mm) for the 10 studied alpine species.

965 **Table 1**

Species	Common name	Life form	Succession	Family
Epilobium fleischeri Hochst.	Alpine willowherb	Forb	Early	Omagraceae
Trisetum distichophyllum (Vill.) P.Beauve.	Tufted hairgrass	Graminoid	Early	Poaceae
Trifolium pallescens Schreb.	Pale clover	Forb	Early	Fabaceae
Luzula spicata (L.) DC.	Spiked woodrush	Graminoid	Mid	Juncaceae
Silene exscapa All.	Moss campion	Forb	Mid	Caryophyllaceae
Minuartia recurva (All.) Schinz and Thell.	Recurved sandwort	Forb	Late	Caryophyllaceae
Festuca halleri All.	Haller's Fescue	Graminoid	Late	Poaceae
Poa laxa Haenke	Banff Bluegrass	Graminoid	Ubiquitous	Poaceae
Salix helvetica Vill.	Swiss willow	Dwarf shrub	Ubiquitous	Salicaceae
Leucanthemopsis alpina (L.) Heyw.	Alpine Moon Daisy	Forb	Ubiquitous	Asteraceae

966

967

968

969 **Table 2** Scanning parameters for X-ray CT.

Voltage (kV)	Current (µA)	Number of projections	Exposure time (ms)	Resolution (µm)	Signal averaging	Total scanning time
180	160	2160	250	54	4/1	2h17min

970

971 **Table 3** Values of root traits analyzed with RooTrak (volume, area, maximum vertical
972 and horizontal length of the root system, convex hull), ImageJ (maximum vertical and
973 horizontal length of the root system) and WinRHIZO (total root length and average
974 root diameter) of the X-ray CT scanned samples.

Plant species	Root type	RooTrak					ImageJ	
		Volume (mm^3) (total mass of the root system)	Area (mm^2) (root area in direct contact with the soil)	Depth (mm) (root system's maximum vertical distance)	Width (mm) (root system's maximum horizontal distance)	Convex hull (mm^2) (region of soil explored by the root system)	Vertical length (mm)	Horizontal length (mm)
T. distichophyllum	Cylindrical	353	3399	63	68	65774	75	7
E. fleischeri	Pole	967	3711	105	65	90931	115	7
T. pallescens	Cone↑	1530	7752	132	72	505364	225	7
S. exscapa	Cone↑	385	2383	102	70	357053	173	6
L. spicata	Cone↓	306	2106	39	71	27046	137	7
F. halleri	Cone↓	828	5866	67	71	60318	107	5
M. recurva	Discoid	144	1677	44	68	60237	164	5
P. laxa	Cone↓	150	1547	33	72	45612	119	3
L. alpina	Umbrella	542	4666	126	72	224012	141	6
S. helvetica	Discoid	435	1146	35	73	24117	49	3

975

976 **Table 4** Plant height (mm), rooting depth (mm) measured with ImageJ, total root
977 length (m), mean root diameter (mm) and root length density (cm cm^{-3}) of the 10
978 studied alpine species measured with WinRHIZO.

Plant species	Plant height (mm)	Rooting depth (mm)	Total root length (m)	Mean root diameter (mm)	Root length density (cm cm^{-3})
T. distichophyllum	50	133	336.9	0.21	85
E. fleischeri	65	197	75.3	0.23	9
T. pallescens	47	133	197.6	0.47	33
S. exscapa	20	153	106.2	0.33	49
L. spicata	30	117	202.1	0.22	81
F. halleri	32	101	297.8	0.35	59
M. recurva	15	118	135.9	0.32	29
P. laxa	51	119	210.1	0.28	47
L. alpina	20	127	368.5	0.26	53
S. helvetica	25	90	342.3	0.27	68

979

980 **Table 5** Root length distribution (%) of the 10 pioneer alpine plants in relation to
981 different diameter classes (mm).

	0<L<0.1	0.1<L<0.2	0.2<L<0.3	0.3<L<0.4	0.4<L<0.5	0.5<L<0.75	0.7
T. distichophyllum	33	41	15	5	2	1	
T. pallescens	49	19	10	5	4	6	
S. exscapa	42	30	12	5	3	4	
L. spicata	57	27	9	3	1	1	
F. halleri	37	22	15	8	5	7	
M. recurva	36	30	13	6	3	5	
P. laxa	49	19	12	6	4	5	
L. alpina	36	29	14	7	5	5	
S. helvetica	9	25	37	6	4	4	

982

983 **Table 6** Life forms, the number of samples (n) tested, the range of root diameters
984 (mm), root tensile strength (MPa) values, scale factor (α) rate of strength decrease
985 (β) and the goodness of fit (R^2) of the 10 studied alpine species.

Species	Life form	n	*d* range (mm)	Mean Tr (MPa)	α	β	R^2	p
T. distichophyllum	Graminoid	30	0.05-1.15	86	23.26	0.62	0.56	<0.001
E. fleischeri	Forb	32	0.04-1.56	58	3.61	1.15	0.67	<0.001
T. pallescens	Forb	32	0.05-1.66	44	10.55	0.88	0.65	<0.001
S. exscapa	Forb	30	0.03-1.14	54	11.85	0.84	0.65	<0.001
L. spicata	Graminoid	30	0.03-0.37	138	9.54	1.01	0.71	<0.001
F. halleri	Graminoid	30	0.05-0.46	94	17.92	0.75	0.70	<0.001
M. recurva	Forb	30	0.03-0.35	60	6.24	1.11	0.78	<0.001

P. laxa	Graminoid	30	0.03-0.56	113	21.65	0.75	0.82	<0.001
L. alpina	Forb	32	0.05-0.59	29	8.67	0.75	0.71	<0.001
S. helvetica	Dwarf shrub	30	0.03-0.78	110	11.34	0.94	0.78	<0.001

Table 7 ANOVA table with multiple comparisons of root tensile strength (MPa) between the studied plant species.

Figure1 a - j Root architecture of the 10 studied pioneer alpine species detected by X-ray CT scanning. a., *E. fleischeri*; b., *F. halleri*; c., *L. alpine*; d., *L. spicata*; e., *M. recurva*; f., *P. laxa*; g., *S. helvetica*; h., *S. exscapa*; i., *T. pallescens*; j., *T. distichophyllum*; Scale bars: a., 35 mm, b., 25 mm, c., 40 mm, d., 15 mm, e., 10 mm, f., 15 mm, g., 15 mm, h., 30 mm, i., 45 mm, j., 20 mm.

a., *E. fleischeri* b., *F. halleri*

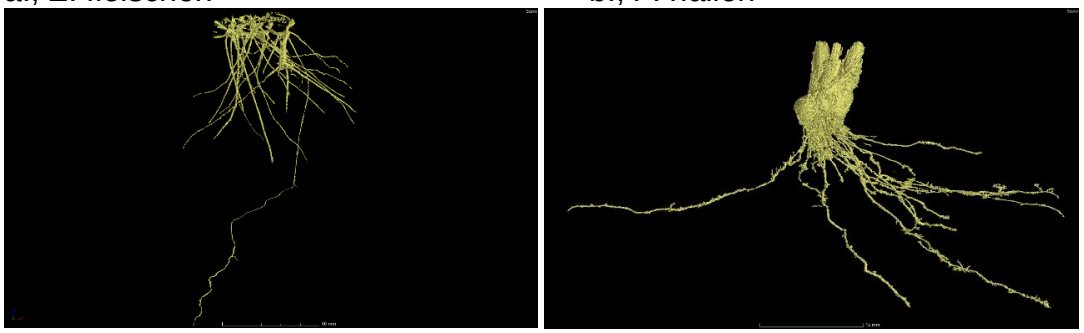

c., *L. alpina* d., *L. spicata*

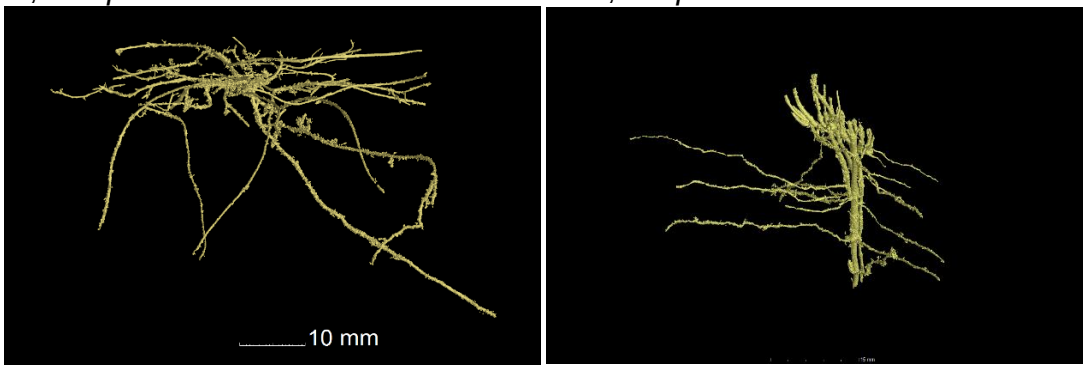

e., *M. recurva* f., *P. laxa*

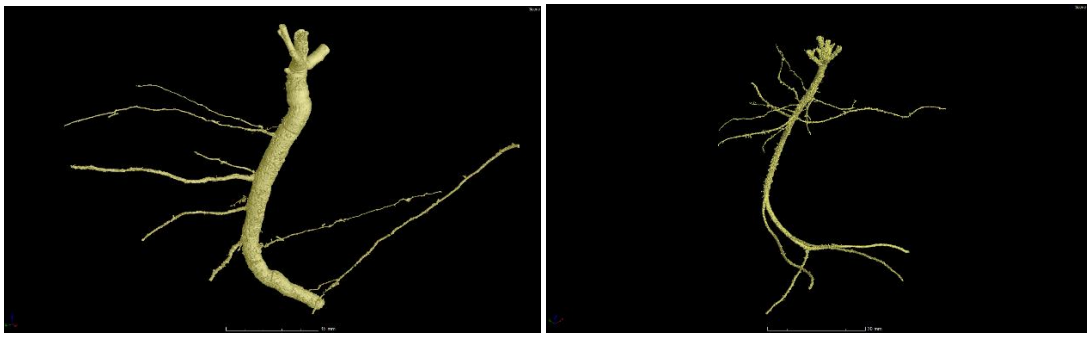

g., *S. helvetica* h., *S. exscapa*

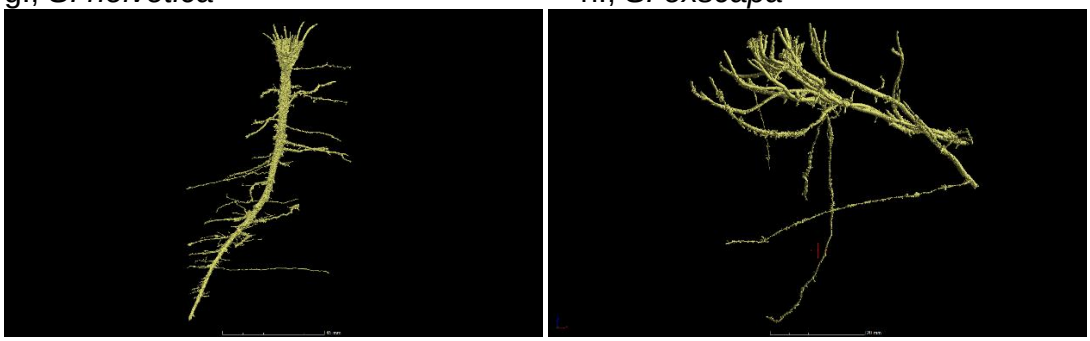

i., *T. pallescens* j., *T. distichophyllum*

Figure 2 *a.,* Image of the cored root system *b.,* the core root system in relation to the soil matrix and *c.,* the washed entire root system of *Trifolium pallescens*. Scale bar a., 45 mm b., 40 mm and c., the ruler uses cm.

a., b., c.,

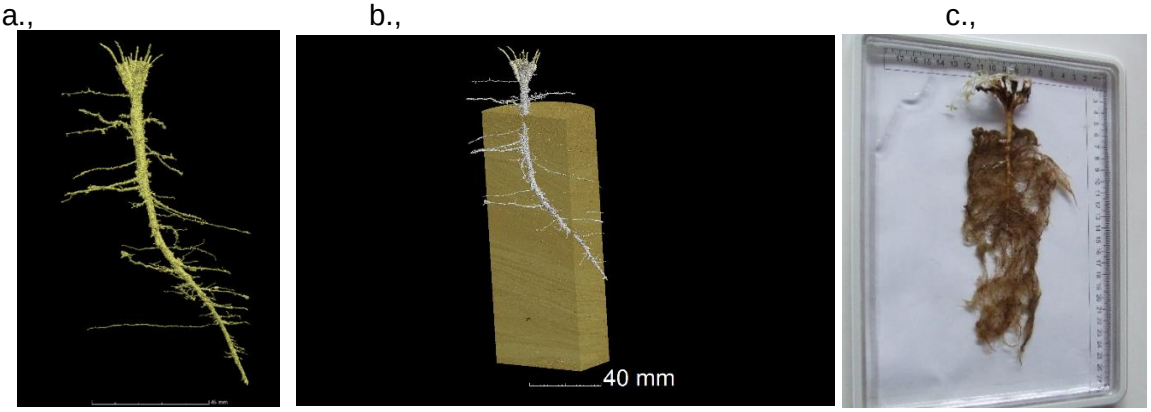

Figure 3 *a.,* Linear correlation between RooTrak and ImageJ data on the maximum vertical and *b.,* horizontal root length for the 10 studied alpine species.

a., b.,

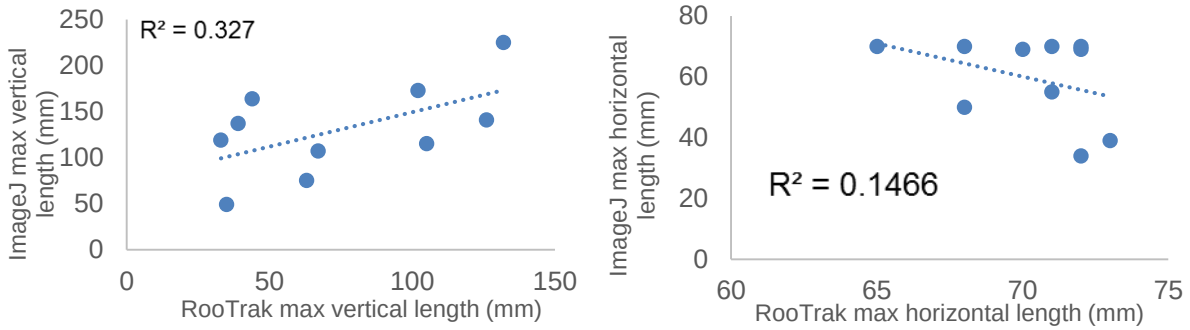

Figure 4

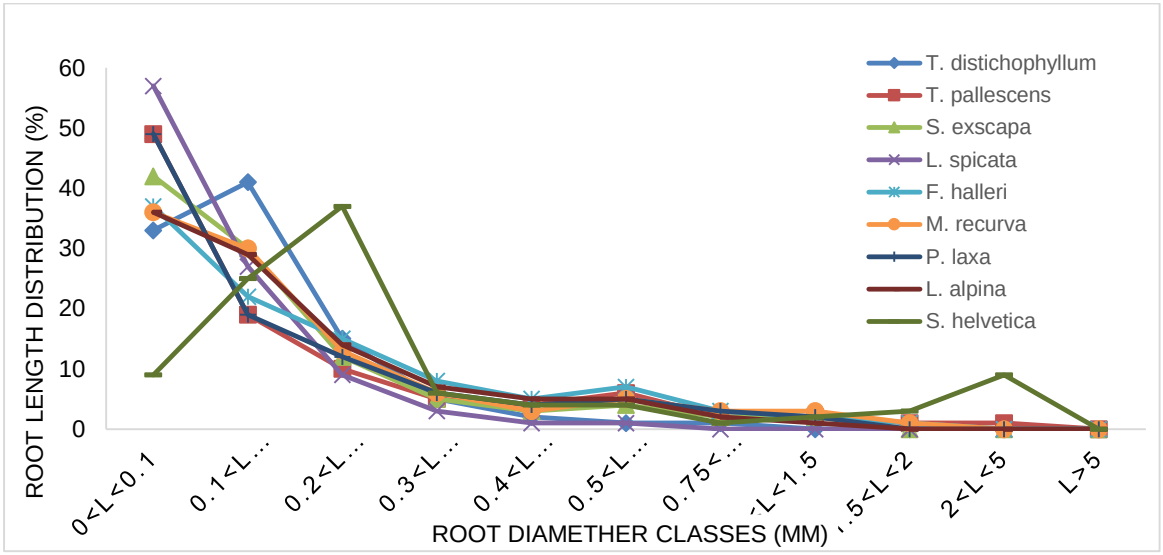

Figure 5 Examples of the grayscale CT images of the soil matrices *a.,* glacial till with *T. distichophyllum b.,* and *c.,* fluvio-glacial and lake depositions.

a., b., c.,

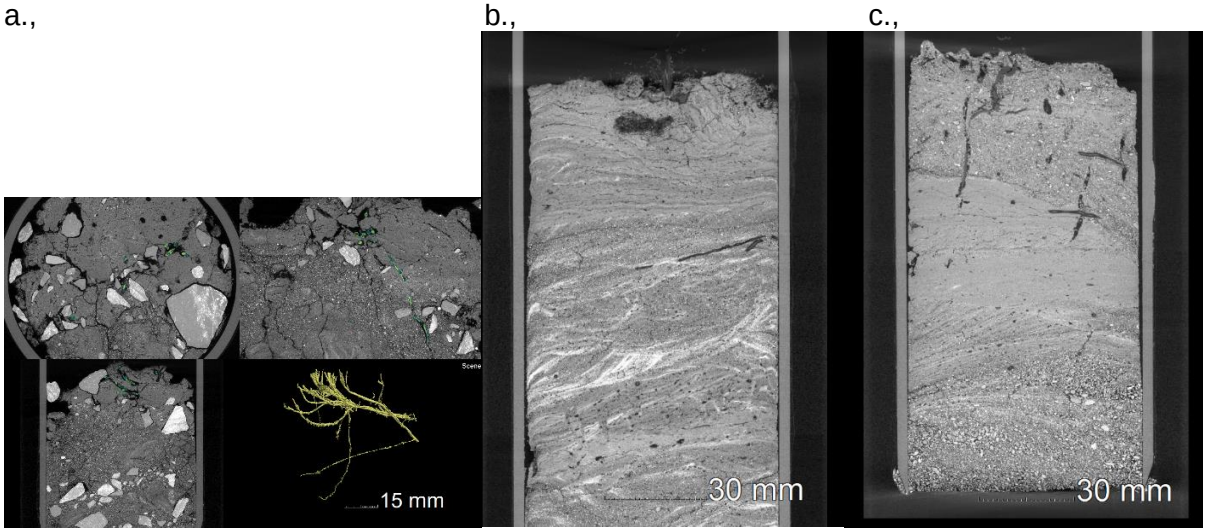

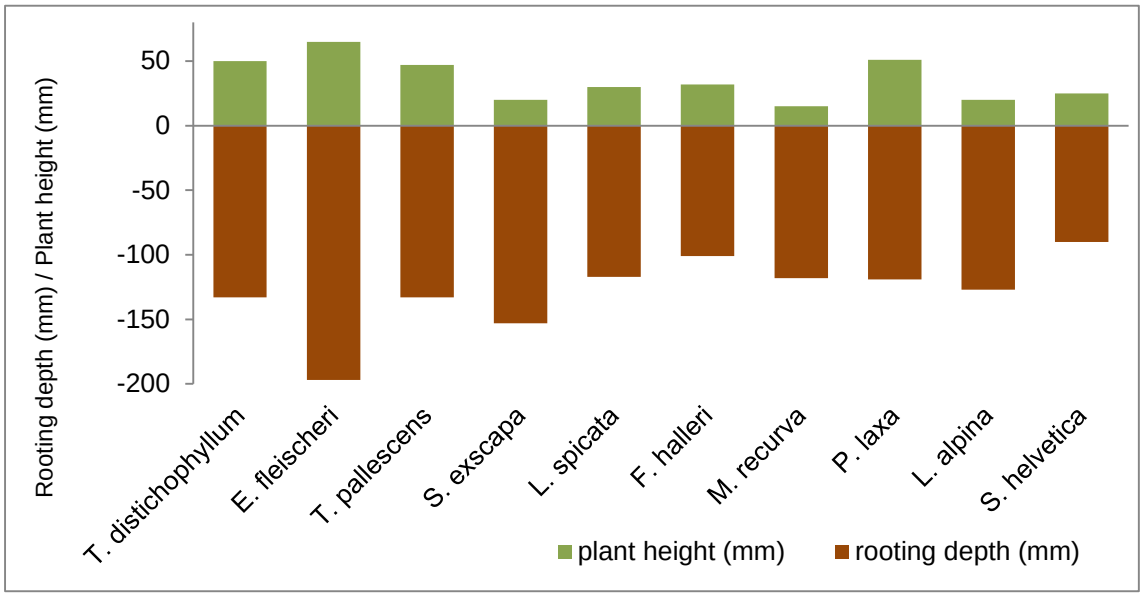

Figure 6 Plant height (cm) and rooting depth (cm) of the 10 studied alpine plant species.

Figure 7 The relationship between root tensile strength (MPa) and root diameter (mm) for the 10 studied alpine species

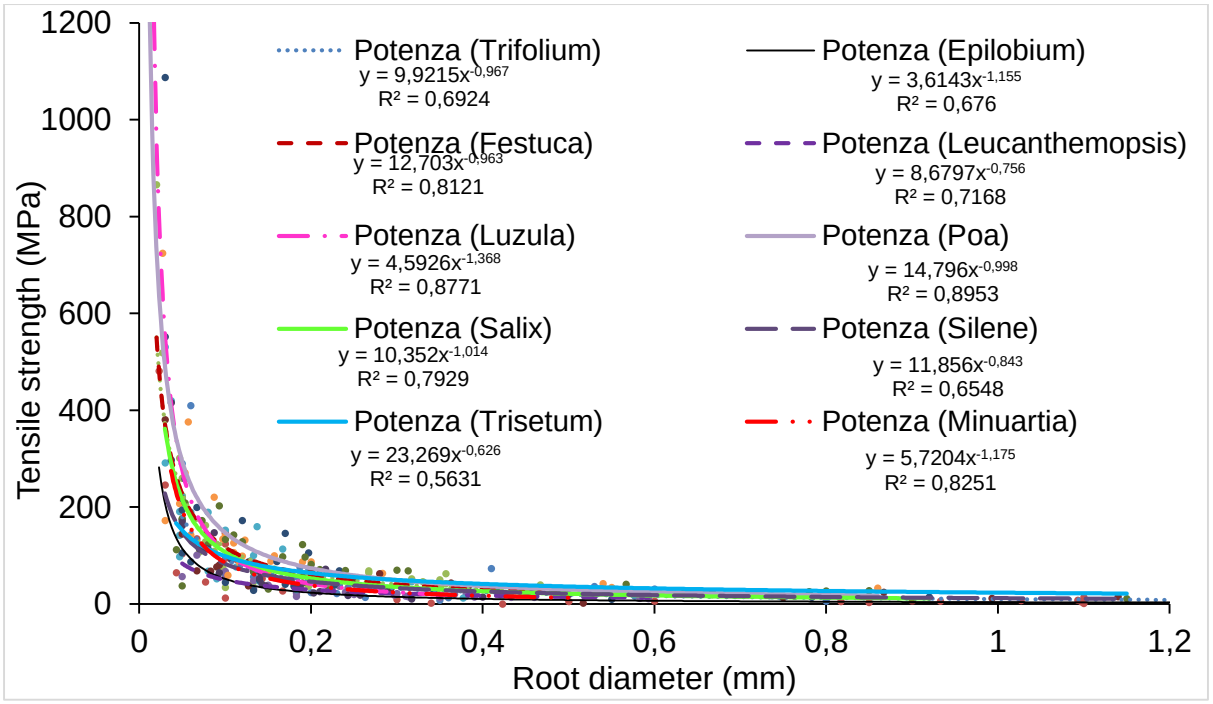
Tensile strength (MPa)
Root diameter (mm)
Potenza (Trifolium)
y = 9,9215x-0,967
R² = 0,6924
Potenza (Epilobium)
y = 3,6143x-1,155
R² = 0,676
Potenza (Festuca)
y = 12,703x-0,963
R² = 0,8121
Potenza (Leucanthemopsis)
y = 8,6797x-0,756
R² = 0,7168
Potenza (Luzula)
y = 4,5926x-1,368
R² = 0,8771
Potenza (Poa)
y = 14,796x-0,998
R² = 0,8953
Potenza (Salix)
y = 10,352x-1,014
R² = 0,7929
Potenza (Silene)
y = 11,856x-0,843
R² = 0,6548
Potenza (Trisetum)
y = 23,269x-0,626
R² = 0,5631
Potenza (Minuartia)
y = 5,7204x-1,175
R² = 0,8251

1033

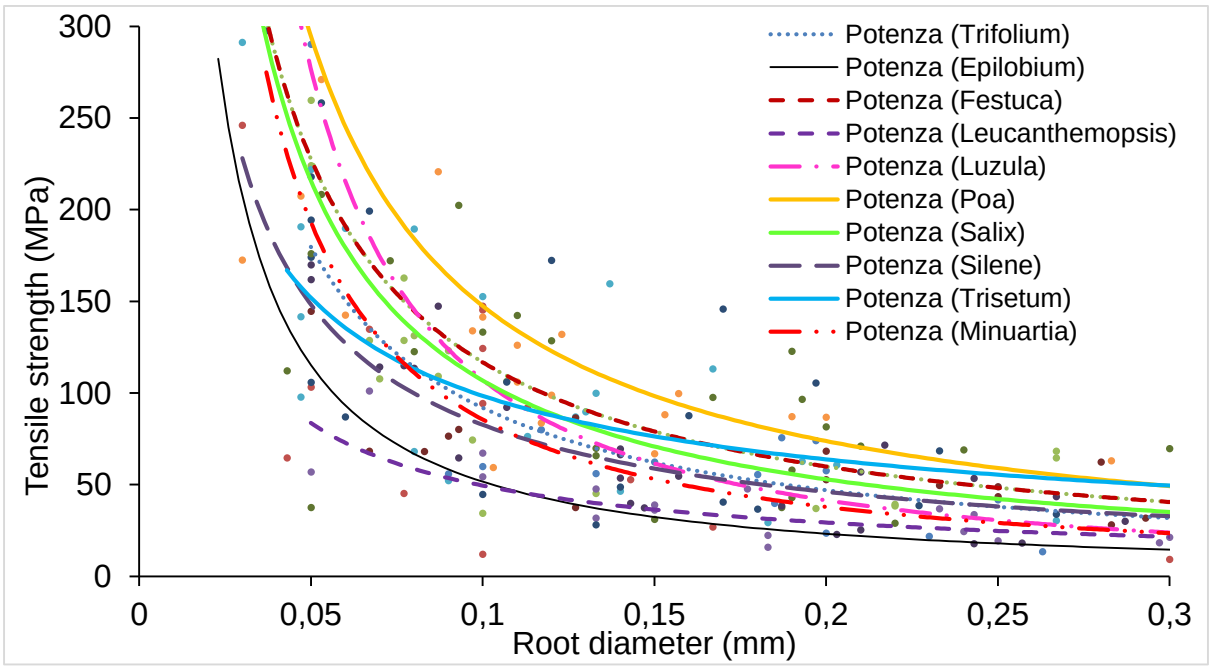
Tensile strength (MPa)
Root diameter (mm)
Potenza (Trifolium)
Potenza (Epilobium)
Potenza (Festuca)
Potenza (Leucanthemopsis)
Potenza (Luzula)
Potenza (Poa)
Potenza (Salix)
Potenza (Silene)
Potenza (Trisetum)
Potenza (Minuartia)

1034